Spontaneous Reduction by One Electron on Water Microdroplets Facilitates Direct Carboxylation with CO₂

Huan Chen,^{1,2} Ruijing Wang,^{1,2} Jinheng Xu,^{1,2,3} Xu Yuan,^{1,2} Dongmei Zhang,^{1,2} Zhaoguo Zhu,³ Mary Marshall,³ Kit Bowen,^{*,3} and Xinxing Zhang^{*,1,2}

¹College of Chemistry, Key Laboratory of Advanced Energy Materials Chemistry (Ministry of Education), Renewable Energy Conversion and Storage Centre, Tianjin Key Laboratory of Biosensing and Molecular Recognition, Frontiers Science Centre for New Organic Matter, Nankai University, Tianjin, 300071, China.

²Haihe Laboratory of Sustainable Chemical Transformations, Tianjin, 300192, China.

³Department of Chemistry, Johns Hopkins University, Baltimore, Maryland, 21218, United States.

*Emails: kbowen@jhu.edu; zhangxx@nankai.edu.cn

ABSTRACT: Recent advances of microdroplet chemistry have shown that chemical reactions in water microdroplets can be accelerated by several orders of magnitude compared to the same reactions in bulk water. Among the large plethora of unique properties of microdroplets, an especially intriguing one is the strong reducing power that can be sometimes as high as alkali metals as a result of the spontaneously generated electrons. In this study, we design a catalyst-free strategy that takes advantage of the reducing ability of water microdroplets to reduce a certain molecule, and the reduced form of that molecule can convert CO_2 into value-added products. By spraying the water solution of C_6F_5I into microdroplets, an exotic and fragile radical anion, $C_6F_5I^{-}$, is observed, where the excess electron counter-intuitively locates on the σ^* antibonding orbital of the C-I bond as evidenced by anion photoelectron spectroscopy. This electron weakens the C-I bond and causes the formation of $C_6F_5^{-}$, and the latter attacks the carbon atom on CO_2 , forming the pentafluorobenzoate product, $C_6F_5CO_2^{-}$. This study provides a good example of strategically making use of the spontaneous properties of water microdroplets, and we anticipate that microdroplet chemistry will be a green avenue rich in new opportunities in CO_2 utilization.

Introduction

The atmospheric carbon dioxide (CO₂) level has exceeded 400 ppm.[1] Current and projected CO2 emissions from anthropogenic activities are leading to a continued rise in global temperatures and sea levels.[2-4] Converting CO₂ into value-added products promises to alleviate the problem, [5-7] but the challenges are obvious since CO₂ is a highly stable molecule with a high C-O bond dissociation energy (525.9 kJ/mol^[8]) and a high ionization potential (317.7 kJ/mol^[9]), so the direct cleavage of the C-O bond or the oxidation by one electron are both difficult. The carbon atom in CO₂ is in the highest oxidation state (+IV), as a result, it can only be activated by its reduction. Nevertheless, the direct attachment of an electron to CO₂ is also challenging, because CO₂ has a large highest-occupied molecular orbital (HOMO) - lowest unoccupied molecular orbital (LUMO) gap, making the occupation of the LUMO by an electron energetically unfavourable, and the electron affinity (EA) of CO₂ is negative (-o.6 eV).[10] So the CO₂ anion is metastable with a short lifetime of ~90 microseconds.[10,11] As a result, despite being highly reactive, the direct use of CO₂. for further CO₂ fixation has been difficult and scarce. [12] Instead of directly using electrons, another

strategy is to use anions or partial negative charges to attack the carbon atom on CO₂, yielding stable products with carboxylic groups.^[13-20]

In recent years, water microdroplet chemistry has emerged as an exciting new field because of its abilities to accelerate chemical reactions by several orders of magnitude compared to the same reactions in bulk water. [21,22] Among the unique properties of water microdroplets, an especially useful one is the observation that water microdroplets exhibit strong reducing power that can be as high as alkali metals.[23] The power of water microdroplets to promote reduction chemistry has been demonstrated in the reduction of dissolved chloroauric acid to yield gold nanoparticles and nanowires,[24] the reduction of doubly charged ethyl viologen to singly charged ethyl viologen, [25] the reduction of organic compounds by hydrogenation, [26] and the formation of pyridyl anion in spraying an aqueous solution containing dissolved pyridine to form microdroplets.^[23] It is postulated that there is a high electric field (109 V/m) at the surface of microdroplets that can pull electrons out of hydroxide ions,[27-30] resulting in an electron and a hydroxyl radical, and the electron is responsible for the above-mentioned reduction reactions, [23-26] and the hydroxyl radical can cause oxidation reactions.[31,32] In some

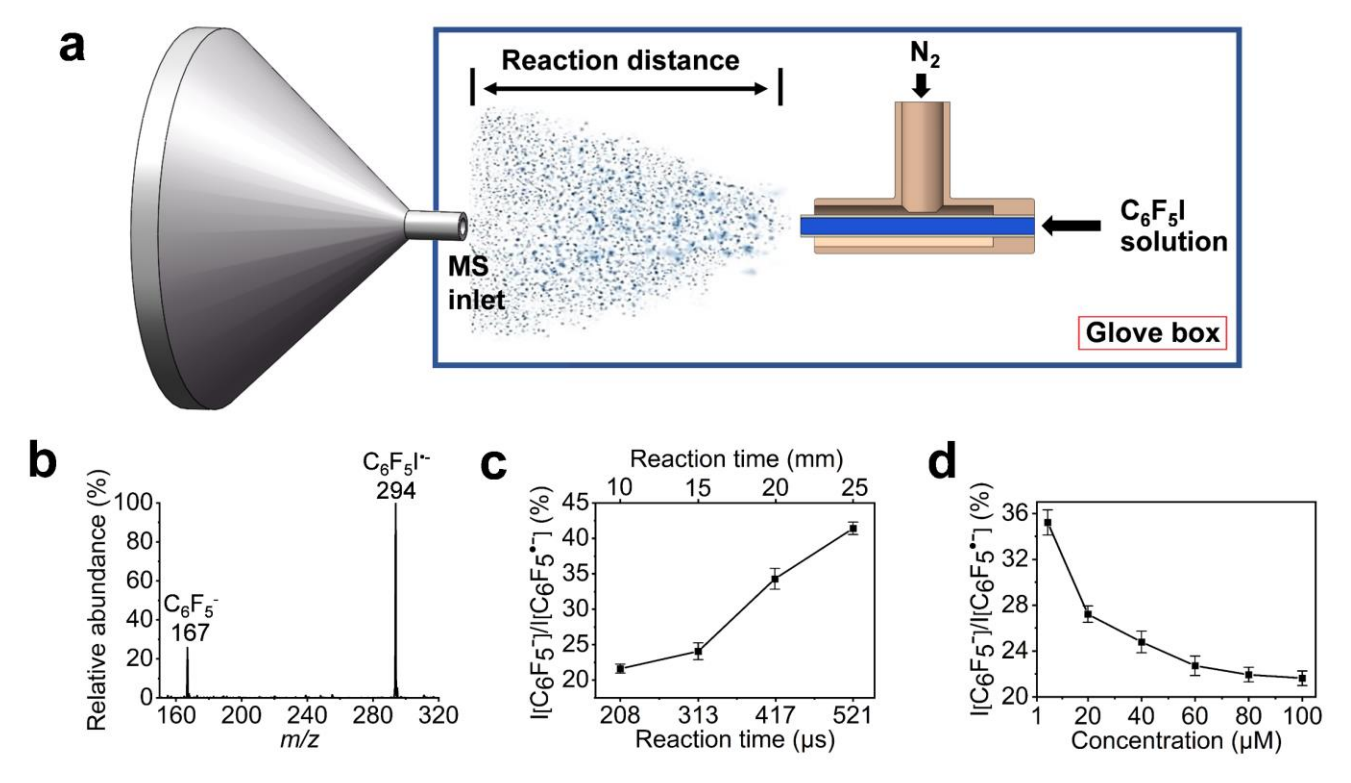


Figure 1. Spontaneous reduction of C_6F_5I in water microdroplets. (a) The experimental setup of the sprayer in a glove box filled with pure N_2 . (b) A typical mass spectrum showing the spontaneous reduction products, $C_6F_5I^{\bullet}$ and $C_6F_5^{-}$. (c) $I[C_6F_5^{-}]/I[C_6F_5I^{\bullet}]$ as a function of the reaction distance and reaction time when the C_6F_5I concentration is 100 μ M and sheath gas pressure is 60 psi. (f) $I[C_6F_5^{-1}]/I[C_6F_5I^{\bullet}]$ as a function of C_6F_5I concentration when the reaction distance is 10

cases, reduction and oxidation reactions occurred simultaneously. [23] The redox potential at the air-water interface has been shown to be very different from the bulk, [33] and a recent study [34] shows that on the aerial surface of air bubbles in water, the oxidation potential of OH- to OH occurs is at least 0.7 V below redox tabled values due to the electrostatic destabilization of the hydroxide anion on water, which accelerates the formation of electrons and hydroxyl radicals at the air-water interface.

In view of the above advances, the spontaneous and strong reducing power of water microdroplets should be able to reduce and fixate CO₂. Previous studies showed that water microdroplet could convert CO2 into formate with or without the addition of triazole as a catalyst. [35,36] In this study, we take advantage of the reducing power of water microdroplets to generate an exotic radical anion of iodopentafluorobenzene (C₆F₅I⁻) by simply spraying the water solution of C₆F₅I into microdroplets in a N₂-filled glove box. To reveal the electronic nature of this anion, a combination of gas-phase anion photoelectron spectroscopy (PES) and theoretical calculation show that the excess electron of $C_6F_5I^-$ locates on the σ^* antibonding orbital of the C-I bond, unlike most radical anions with benzene rings whose excess electrons prefer to be on the π^* antibonding orbital. The electron weakens the C-I bond of C₆F₅I and forms the C_6F_5 anion, and the latter attacks the carbon atom on CO_2 , forming the pentafluorobenzoate product, C₆F₅CO₂. This study brings a new strategy of CO₂ fixation by converting a molecule into its reduced form by water microdroplets,

which further promotes carboxylation by attacking the C atom on CO₂.

Results and discussion

Detailed experimental methods are provided in the Supporting Information (SI). Fig. 1a presents the experimental setup. The water solutions of C₆F₅I with different concentrations are forced by a syringe pump through a fused silica capillary that sits inside a larger coaxial capillary through which high pressure N2 sheath gas flows. The resulting spray of microdroplets is aimed toward the inlet of a mass spectrometer. The mass spectrometer's inlet is inserted into a glove box filled with pure N₂ (Fig. 1a). [37] The distance between the end of the sprayer and the mass spectrometer inlet is defined as the microdroplet flying (reaction) distance.[38] Fig. 1b presents a mass spectrum showing the spontaneous reduction products by spraying water solutions of C₆F₅I into water microdroplets. Two anionic products, $C_6F_5I^{\bullet-}$ (m/z = 294) and $C_6F_5^{--}$ (m/z = 167), were observed. Apparently C₆F₅I was reduced by one electron into a radical anion, supporting the fact that electrons can easily be generated in microdroplets, and the C₆F₅- anion could be a C-I bond dissociation product from C₆F₅I^{•-} via a dissociative electron attachment (DEA) process. [39] A same experiment performed in the atmosphere did not yield any signal related to C_6F_5I , suggesting that $C_6F_5I^{\bullet-}$ is a fragile anion that cannot survive air. To provide evidence that C₆F₅⁻ was indeed a product from C₆F₅I^{•-} through C-I bond dissociation, Fig. 1c shows the change of $I[C_6F_5]/I[C_6F_5I^{\bullet-}]$

as a function of the reaction distance and reaction time, where I denotes the mass peak intensity. By adjusting the reaction distance from 10 to 25 mm, the reaction time varied from 208 to 521 μ s^[38] (Fig. 1c), and a clear increase of the ratio was observed, indicating that the airborne microdroplet, but not the gas phase inside the mass spectrometer, was where the reaction occured, and that $C_6F_5^-$ was a product from C₆F₅I[•]. The reaction kinetics was also dependent on the concentration of C₆F₅I (Fig. 1d). A higher $I[C_6F_5]/I[C_6F_5I^{\bullet-}]$ ratio was observed with a lower concentration. In a model study by Wilson and coworkers, [40] lower concentrations yielded higher fractions of the molecules partitioning to the microdroplet surface, suggesting that the air-water interface of the microdroplets played a key role in the reactions, which is consistent with this case and our previous studies. [25,28] The mass spectra supporting the data in Fig. 1c and 1d are displayed in Fig. S1 and S2, respectively, and the collision-induced dissociation (CID) spectra bearing structural information of these species are provided in Fig. S3.

To understand the geometric and electronic structures of $C_6F_5I^{\bullet}$ and $C_6F_5^{\bullet}$, we also performed gas-phase PES measurements and density functional theory (DFT) calculations. Detailed methods are provided in the SI. Briefly, a home-built apparatus combines a laser photoemission ion source, time-of-flight (TOF) mass spectrometry and anion PES. We analysed the kinetic energies of the resultant photoelectrons by crossing a mass-selected anion beam with a fixed-frequency photon beam. The energetics of the photodetachment process are governed by the energy-conserving relationship, hv = EBE + EKE, where hv is the photon energy, EBE is the electron binding (photodetachment transition) energy, and EKE is the electron kinetic energy. Fig. 2 presents the photoelectron spectra of C₆F₅-, I- and $C_6F_5I^{\bullet-}$ taken with different photon energies. The spectrum of C₆F₅ in Fig. 2a exhibits an EBE band starting from around 3.05 eV and peaking at 3.53 eV, these two values corresponding to the EA of C_6F_5 and vertical detachment energy (VDE) of C₆F₅, in consistent with our calculated values, 3.18 eV and 3.50 eV, at the PBE/aug-cc-pVTZ level of theory. The spectrum of I- in Fig. 2b shows a sharp peak at 3.06 eV, corresponding to the well-known EA of iodine.[41] Fig. 2c exhibits the PES of the C₆F₅I• parent anion using 266 nm photons. The first band starts from ~2.5 eV and peaks at 3.05 eV (VDE). The measured VDE agrees well with the calculated value, 3.12 eV at the PBE/aug-ccpVTZ(C,F)/aug-cc-pVTZ-PP(I) level of theory, but the onset of the first band, 2.5 eV, is not consistent with the calculated EA value, 1.59 eV. In PES experiments, only when there is enough Franck-Condon overlap between the ground state of the anion and the ground state of the neutral can EA be observed, [42] suggesting that the observed onset of the C₆F₅I^{•-} spectrum is not the EA due to the lack of Franck-Condon overlap (vide infra). As a result, we can only compare the calculated EA with a previous experiment, 1.48 eV, using a pulsed electron high-pressure mass spectrometer.^[43] In Fig. 2d, the PES of C₆F₅I^{•-} at 355 nm obviously has features from C₆F₅ (black), I⁻ (blue) and C₆F₅I^{•-} (red), which is a result of two-photon processes: the first

photon dissociates $C_6F_5I^{\bullet}$ into either $C_6F_5^{\bullet}$ or I^{\bullet} , and the second photon photodetaches them. The photodissociation suggests that the C-I bond is weakened in $C_6F_5I^{\bullet}$ and vulnerable to 355 nm photons. The experimental and measured EA and VDE values are tabulated in Table 1 for comparisons.

Species	Expt. EA	Theo. EA	Expt. VDE	Theo. VDE
$C_6F_5/C_6F_5^{-1}$	3.05	3.18	3.53	3.50
I/I-	3.06 ^[35]	-	-	-
$C_6F_5I/C_6F_5I^{\bullet \text{-}}$	1.48[37]	1.59	3.05	3.12

Table 1. The experimental and theoretical EA and VDE values. All numbers are in eV.

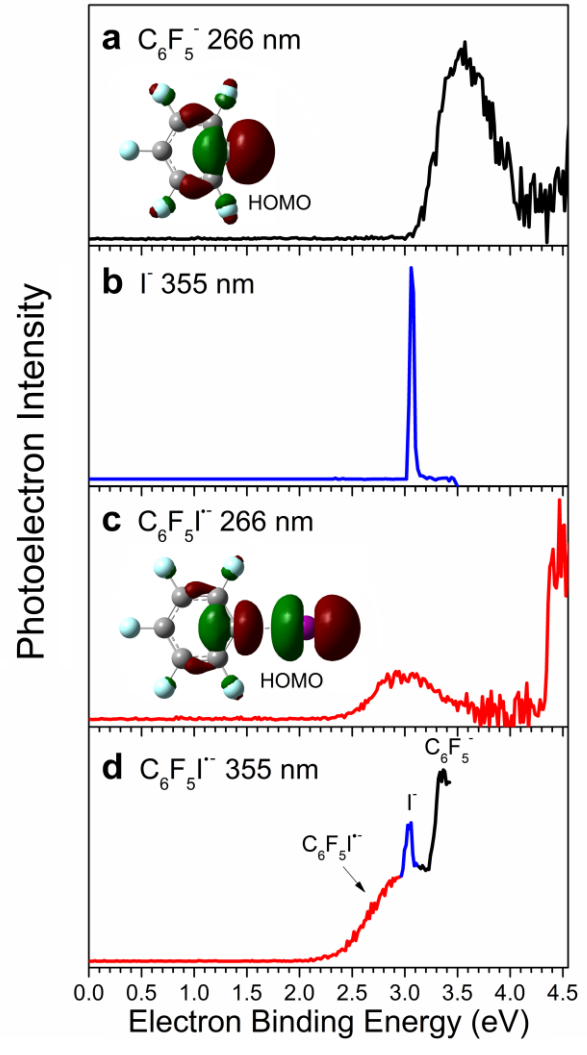


Figure 2. Photoelectron spectroscopic study of the anion species. (a) The spectrum of $C_6F_5^-$ taken with 266 nm photons. (b) The spectrum of I^- taken with 355 nm photons. (c) The spectrum of $C_6F_5I^{\bullet-}$ taken with 266 nm photons. (d) The spectrum of $C_6F_5I^{\bullet-}$ taken with 355 nm photons. The HOMOs of $C_6F_5^-$ and $C_6F_5I^{\bullet-}$ are embedded.

As a side note, the superatom concept depicts a class of clusters and molecules that possess certain behavior akin to an atom of the periodic table. [44] EA was considered to

be the defining characteristic for identifying a superatom of a halogen element. With this criterion, Al_{13} was determined to be the superatom of $Br.^{[45]}$ Since the EA of C_6F_5 and I are almost identical, we opine that C_6F_5 can be viewed as a superatom of I.

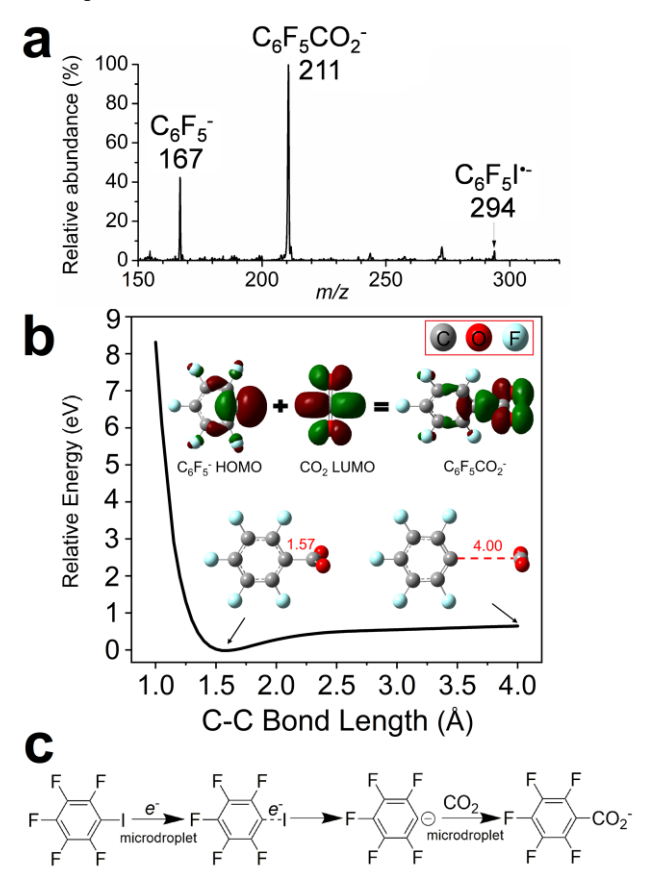


Figure 3.The fixation of CO_2 by $C_6F_5^-$ in microdroplets. (a) A mass spectrum showing the $C_6F_5CO_2^-$ product when using CO_2 as the sheath gas. (b) DFT calculation results of the potential energy surface along the C-C bond of the $(C_6F_5-CO_2)^-$ complex at the PBE/aug-cc-pVTZ level of theory. Typical structures along the scanned coordinate and the frontier orbitals involved in the reactions are displayed. (c) The overall reaction pathway.

The calculated HOMOs of $C_6F_5^-$ and $C_6F_5I^{\bullet-}$ are embedded in Fig. 2. Unlike most radical anions with benzene rings where the excess electrons prefer to be on the π^* antibonding orbital on the ring, the excess electron of $C_6F_5I^{--}$ locates on the σ^* antibonding orbital of the C-I bond, which is a singly occupied molecular orbital (SOMO), making it a half bond, and elongating it from 2.09 Å to 2.67 Å. Such a large bond length change from neutral to anion causes a poor Franck-Condon overlap, explaining the failure of the measurement of EA in the PES experiment. This result also explains the formation of $C_6F_5^-$ by breaking the weakened C-I bond. The HOMO of $C_6F_5^-$ is an occupied sp^2 orbital locating on the carbon atom, making it negatively charged by -0.38 e (Fig. S4), providing a chance for attacking the carbon atom on the CO_2 molecule. The calculated

geometric and charge information of these species are provided in Fig. S₄, and the Cartesian coordinates of all the calculated species are provided in Table S₁.

We next move to the CO₂ fixation experiment taking advantage of the reducing power of water microdroplets. Fig. 3a shows the mass spectrum using CO₂ as the sheath gas, and a new peak corresponding to the pentafluorobenzoate product, C₆F₅CO₂-, is unambiguously observed. Remarkably, there were $\sim 71\%$ of the C_6F_5 anions converted into $C_6F_5CO_2$. The signal of $C_6F_5I^{\bullet-}$ become very low, suggesting that the formation of C₆F₅CO₂ was a channel consuming C_6F_5 , and C_6F_5 comes from $C_6F_5I^{\bullet}$. To better understand the reaction pathway, we performed DFT calculations at the PBE/aug-cc-pVTZ level of theory. Fig. 2B plots the potential energy surface for the (C₆F₅-CO₂)- complex as a function of the C-C bond length with the remainder of the molecule relaxed to the ground state. There is only one potential well along the C-C coordinate, meaning that this is a barrier-free reaction. Due to the steric hindrance, the C_6F_5 moiety and the CO_2 moiety are not in the same plane. The well corresponds to the fully optimized structure with a C-C bond length of 1.57 Å. As shown in the embedded figure in Fig. 3b, the symmetry of C₆F₅- HOMO matches that of CO2 LUMO, explaining the barrier-free formation of the C-C bond. However, since the energy well is not large (~1 eV), one expects this reaction to be endergonic in the gas phase due to unfavorable entropic contributions, so solvation effects in the microdroplets might have considerably stabilized the C₆F₅CO₂ product. The overall strategy of fixating CO₂ is provided in Fig. 3c, and the key step is apparently using microdroplet as a green and spontaneous electron donor.

Conclusion

To summarize, we have used spontaneously generated electrons in water microdroplets to reduce C_6F_5I into $C_6F_5I^{\bullet}$, where the excess electron unusually occupies the σ^* antibonding orbital of the C-I bond and further breaks the bond, forming the $C_6F_5^-$ anion that fixates CO_2 into $C_6F_5CO_2^-$. This study provides an example of CO_2 utilization, and brings a new catalyst-free strategy that takes advantage of the reducing power of water microdroplets for the applications of not only CO_2 fixation, but also potentially a large variety of reactions such as reductive coupling and hydrogenation where the reduction by an electron plays the key role.

ASSOCIATED CONTENT

Supporting Information.

This material is available free of charge via the Internet at http://pubs.acs.org.

Experimental and theoretical methods. Figures S1-S4 and Table S1 showing additional experimental and theoretical results.

Notes

The authors declare no competing financial interests.

ACKNOWLEDGMENT

X.Z. acknowledges the National Natural Science Foundation of China (22174073 & 22003027), the NSF of Tianjin City (21JCJQJC00010), the Haihe Laboratory of Sustainable Chemical Transformations, the Beijing National Laboratory for Molecular Sciences (BNLMS202106), and the Frontiers Science Center for New Organic Matter at Nankai University (63181206). Portions of this material are based on work supported by the US National Science Foundation (NSF) under grant number CHE-2054308 (K.H.B.).

REFERENCES

- (1) Hartfield, G. et. al. State of the Climate in 2017. Bull. Am. Meteorol. Soc. 2018, 99, Si-S310.
- (2) Brown, P. T.; Caldeira, K. Greater Future Global Warming Inferred from Earth's Recent Energy Budget. *Nature* **2017**, *552*, 45-50.
- (3) Cox, P. M.; Betts, R. A.; Jones, C. D.; Spall, S. A.; Totterdell, I. J. Acceleration of Global Warming due to Carbon-Cycle Feedbacks in a Coupled Climate Model. *Nature* **2000**, *408*, 184-187.
- (4) Joos, F.; Plattner, G. K.; Stocker, T. F.; Marchal, O.; Schmittner, A. Global Warming and Marine Carbon Cycle Feedbacks an Future Atmospheric CO₂. *Science* **1999**, 284, 464-467.
- (5) Jiang, X.; Nie, X. W.; Guo, X. W.; Song, C. S.; Chen, J. G. G. Recent Advances in Carbon Dioxide Hydrogenation to Methanol via Heterogeneous Catalysis. *Chem. Rev.* **2020**, *120*, *7984-8034*.
- (6) Grignard, B.; Gennen, S.; Jerome, C.; Kleij, A. W.; Detrembleur, C. Advances in the Use of CO₂ as a Renewable Feedstock for the Synthesis of Polymers. *Chem. Soc. Rev.* **2019**, *48*, 4466-4514.
- (7) Wang, G. X.; Chen, J. X.; Ding, Y. C.; Cai, P. W.; Yi, L. C.; Li, Y.; Tu, C. Y.; Hou, Y.; Wen, Z. H.; Dai, L. M. Electrocatalysis for CO₂ Conversion: from Fundamentals to Value-added Products. *Chem. Soc. Rev.* **2021**, *50*, 4993-5061.
- (8) Darwent, B. deB. Bond Dissociation Energies in Simple Molecules; National Bureau of Standards: Washington, DC, 1970.
- (9) Lias, S. G. Ionization Energy Evaluation. *In NIST Chemistry WebBook*; Mallard, W. G., Linstrom, P. J., Eds.; NIST Standard Reference Database Number 69; National Institute of Standards and Technology: Gaithersburg, MD, 2017.
- (10) Compton, R. N.; Reinhardt, P. W.; Cooper, C. D. Collisional Ionization of Na, K, and Cs by CO₂, COS, and CS₂: Molecular Electron Affinities. *J. Chem. Phys.* **1975**, *6*3, 3821.
- (11) Yu, D.; Rauk, A.; Armstrong, D. A. Electron Affinities and Thermodynamic Properties of Some Triatomic Species. *J. Phys. Chem.* **1992**, *96*, 6031–6038.
- (12) Song, L.; Wang, W.; Yue, J.; Jiang, Y.; Wei, M.; Zhang, H.; Yan, S.; Liao, L.; Yu, D. Visible-light Photocatalytic Di- and Hydro-Carboxylation of Unactivated Alkenes with CO₂. *Nat. Catal.* **2022**, 5, 832-838.
- (13) Zhang, X.; Lim, E.; Kim, S. K.; Bowen, K. H. Photoelectron Spectroscopic and Computational Study of (M-CO₂)⁻ Anions, M = Cu, Ag, Au. *J. Chem. Phys.* **2015**, *143*, 174305.
- (14) Liu, G.; Ciborowski, S. M.; Zhu, Z.; Chen, Y.; Zhang, X.; Bowen, K. H. The Metallo-Formate Anions, M(CO₂)-, M = Ni, Pd, Pt, Formed by Electron-Induced CO₂ Activation. *Phys. Chem. Chem. Phys.* 2019, 21, 10955-10960.
- (15) Lim, E.; Heo, J.; Zhang, X.; Bowen, K. H.; Lee, S. H.; Kim, S. K. Anionic Activation of CO_2 via $(M_n-CO_2)^-$ Complex on Magic-Numbered Anionic Coinage Metal Clusters M_n^- (M = Cu, Ag, Au). *J. Phys. Chem. A* **2021**,*125*, 2243–2248.
- (16) Knurr, B. J.; Weber, J. M. Solvent-Driven Reductive Activation of Carbon Dioxide by Gold Anions. *J. Am. Chem. Soc.* **2012**, *134*, 18804-18808.

- (17) Lee, S. H.; Kim, N.; Ha, D. G.; Kim, S. K. "Associative" Electron Attachment to Azabenzene– $(CO_2)_n$ van der Waals Complexes: Stepwise Formation of Covalent Bonds with Additive Electron Affinities. *J. Am. Chem. Soc.* **2008**, *130*, 16241-16244.
- (18) Graham, J. D.; Buytendyk, A. M.; Wang, Y.; Kim, S. K.; Bowen, K. H. CO₂ Binding in the (Quinoline-CO₂)⁻ Anionic Complex. *J. Chem. Phys.* **2015**, *142*, 234307.
- (19) Graham, J. D.; Buytendyk, A. M.; Zhang, X.; Kim, S. K.; Bowen, K. H. Carbon Dioxide Is Tightly Bound in the [Co(Pyridine)(CO₂)]- Anionic Complex. *J. Chem. Phys.* **2015**, *143*, 184315.
- (20) Oh, R.; Lim, E.; Zhang, X.; Heo, J.; Bowen, K. H.; Kim, S. K. Ab Initio Study on Anomalous Structures of Anionic [(N-heterocycle)-CO₂]- Complexes. *J. Chem. Phys.* **2017**, *146*, 134304.
- (21) Yan, X.; Bain, R. M.; Cooks, R. G. Organic Reactions in Microdroplets: Reaction Acceleration Revealed by Mass Spectrometry. *Angew. Chem. Int. Ed.* **2016**, 55, 12960–12972.
- (22) Lee, J. K.; Banerjee, S.; Nam, H. G.; Zare, R. N. Acceleration of Reaction in Charged Microdroplets. *Q. Rev. Biophys.* **2015**, *48*, 437–444.
- (23) Zhao, L.; Song, X.; Gong, C.; Zhang, D.; Wang, R.; Zare, R. N.; Zhang, X. Sprayed Water Microdroplets Containing Dissolved Pyridine Spontaneously Generate Pyridyl Anions. *Proc. Natl. Acad. Sci. U.S.A.* 2022, 119, e220099119.
- (24) Lee, J. K.; Samanta, D.; Nam, H. G.; Zare, R. N. Spontaneous Formation of Gold Nanostructures in Aqueous Microdroplets. *Nat. Commun.* **2018**, *9*, 1562.
- (25) Gong, C.; Li, D.; Li, X.; Zhang, D.; Xing, D.; Zhao, L.; Yuan, X.; Zhang, X. Spontaneous Reduction-Induced Degradation of Viologen Compounds in Water Microdroplets and Its Inhibition by Host–Guest Complexation. *J. Am. Chem. Soc.* **2022**, *144*, 3510–3516.
- (26) Lee, J. K.; Samanta, D.; Nam, H. G.; Zare, R. N. Micrometer-Sized Water Droplets Induce Spontaneous Reduction. *J. Am. Chem. Soc.* **2019**, *141*, 10585–10589.
- (27) Lee, J. K.; Walker, K. L.; Han, H. S.; Kang, J.; Prinz, F. B.; Waymouth, R. M.; Nam, H. G.; Zare, R. N. Spontaneous Generation of Hydrogen Peroxide from Aqueous Microdroplets. *Proc. Natl. Acad. Sci. U.S.A.* 2019, 116, 19294–19298.
- (28) Zhang, D.; Yuan, X.; Gong, C.; Zhang, X. High Electric Field on Water Microdroplets Catalyzes Spontaneous and Ultrafast Oxidative C–H/N–H Cross-Coupling. *J. Am. Chem. Soc.* **2022**, *144*, 16184–16190.
- (29) Mehrgardi, M. A.; Mofidfar, M.; Zare, R. N. Sprayed Water Microdroplets Are Able to Generate Hydrogen Peroxide Spontaneously. *J. Am. Chem. Soc.* **2022**, *144*, 7606–7609.
- (30) Sun, Z. Y.; Wen, X.; Wang, L. M.; Ji, D. X.; Qin, X. H.; Yu, J. Y.; Ramakrishna, S. Emerging Design Principles, Materials, and Applications for Moisture-enabled Electric Generation. *eScience* **2022**, 2, 32-46.
- (31) Xing, D.; Meng, Y.; Yuan, X.; Jin, S.; Song, X.; Zare, R. N.; Zhang, X. Capture of Hydroxyl Radicals by Hydronium Cations in Water Microdroplets. *Angew. Chem. Int. Ed.* **2022**, *61*, e202207587.
- (32) Xing, D.; Yuan, X.; Liang, C.; Jin, T.; Zhang, S.; Zhang, X. Spontaneous Oxidation of I⁻ in Water Microdroplets and Its Atmospheric Implications. *Chem. Commun.* **2022**, *58*, 12447–12450.
- (33) Martins-Costa, M.; Anglada, J.; Francisco, J.; Ruiz-Lopez, M. Reactivity of Atmospherically Relevant Small Radicals at the Air–Water Interface. *Angew. Chem.* **2012**, *51*, 5413–5417.
- (34) Vogel, Y. B.; Evans, C. W.; Belotti, M.; Xu, L.; Russell, I. C.; Yu, L.; Fung, A. K. K.; Hill, N. S.; Darwish, N.; Gonçales, V. R.; Coote, M. L.; Iyer, S. K.; Ciampi, S. The Corona of a Surface Bubble Promotes Electrochemical Reactions. *Nat. Commun.* **2020**, *11*, 6323.
- (35) Song, X.; Meng, Y.; Zare, R. N. Spraying Water Microdroplets Containing 1,2,3-Triazole Converts Carbon Dioxide into Formic Acid. *J. Am. Chem. Soc.* **2022**, *144*, 16744–16748
- (36) Qiu, L.; Cooks, R. G. Simultaneous and Spontaneous Oxidation and Reduction in Microdroplets by the Water Radical Cation/Anion Pair. *Angew. Chem. Int. Ed.* **2022**, *61*, e202210765.

- (37) Zhang, D.; Lu, Y.; Wang, J.; Gong, C.; Hou, X.; Zhang, X.; Chen, J. Revisiting the Hitherto Elusive Cyclohexanehexone Molecule: Bulk Synthesis, Mass Spectrometry, and Theoretical Studies. *J. Phys. Chem. Lett.* **2021**, *12*, 9848-9852.
- (38) Lai, Y.; Sathyamoorthi, S.; Bain, R. M.; Zare, R. N. Microdroplets Accelerate Ring Opening of Epoxides. *J. Am. Soc. Mass Spectr.* **2018**, *29*, 1036-1043.
- (39) Christophorou, L. G.; Stockdale, J. A. D. Dissociative Electron Attachment to Molecules. *J. Chem. Phys.* **1968**, 48, 1956.
- (40) Wilson, K. R.; Prophet, A. M.; Rovelli, G.; Willis, M. D.; Rapf, R. J.; Jacobs, M. I. A Kinetic Description of How Interfaces Accelerate Reactions in Micro-compartments. *Chem. Sci.* **2020**, *11*, 8533-8545.
- (41) Hanstorp, D.; Gustafsson, M. Determination of the Electron Affinity of Iodine. *J. Phys. B: At. Mol. Opt. Phys.* **1992**, 25, 1773.

- (42) Wang, W.; Marshall, M.; Collins, E.; Marquez, S.; Mu, C.; Bowen, K. H.; Zhang X. Intramolecular Electron-Induced Proton Transfer and Its Correlation with Excited-State Intramolecular Proton Transfer. *Nat. Commun.* **2019**, *10*, 1170.
- (43) Dillow, G. W.; Kebarle, P. Substituent Effects on the Electron Affinities of Perfluorobenzenes C_6F_5X . *J. Am. Chem. Soc.* **1989**, 111, 5592-5596.
- (44) Luo, Z.; Castleman, A. W. Special and General Superatoms. *Acc. Chem. Res.* **2014**, 47, 2931-2940.
- (45) Bergeron, D. E.; Castleman, A. W.; Morisato, T.; Khanna, S. N. Formation of Al₃I: Evidence for the Superhalogen Character of Al₃. *Science* **2004**, 304, 84-87.

